EVALUATION OF THE IN VITRO EFFECTOF GOLD NANOROD ASPECT RATIO, SURFACE CHARGE AND CHEMISTRY ON CELLULAR ASSOCIATION AND CYTOTOXICITY

ANTHONY B. POLITO III, Maj, USAF, BSC, PhD, MT(ASCP)SBB

March 2016
Final Report for March 2014 to Dec 2015

REPORT DOCUMENTATION PAGE

Form Approved
OMB No. 0704-0188

1. REPORT DATE *(DD-MM-YYYY)*	2. REPORT TYPE	3. DATES COVERED *(From - To)*
28-03-2016	Final	July 2012 – Jan 2016

4. TITLE AND SUBTITLE
EVALUATION OF THE IN VITRO EFFECT OF GOLD NANOROD ASPECT RATIO, SURFACE CHARGE AND CHEMISTRY ON CELLULAR ASSOCIATION AND CYTOTOXICITY,

5a. CONTRACT NUMBER

5b. GRANT NUMBER

5c. PROGRAM ELEMENT NUMBER

6. AUTHOR(S)
ANTHONY B. POLITO III, Maj, USAF, BSC, PhD, MT(ASCP)SBB

5d. PROJECT NUMBER

5e. TASK NUMBER

5f. WORK UNIT NUMBER

7. PERFORMING ORGANIZATION NAME(S) AND ADDRESS(ES)
Air Force Institute of Technology (AFIT) Civilian Institution Programs (CIP)
2950 Hobson Way
WPAFB OH 45433-7765

8. PERFORMING ORGANIZATION REPORT NUMBER

9. SPONSORING/MONITORING AGENCY NAME(S) AND ADDRESS(ES)
Clinical Investigations
Office of the Air Force Surgeon General SG5M,
Research and Innovations
7700 Arlington Blvd, Ste 5164
Falls Church, VA 22042-5164

10. SPONSOR/MONITOR'S ACRONYM(S)

11. SPONSORING/MONITORING AGENCY REPORT NUMBER

12. DISTRIBUTION AVAILABILITY STATEMENT
Distribution A: Approved for public release; distribution unlimited.

13. SUPPLEMENTARY NOTES

14. ABSTRACT

Gold nanorods (GNRs), due to their unique optical & electronic properties are popular candidates for novel nano-based biomedical applications. Unfortunately, previous studies have reported the potential for GNR cytotoxicity related to the materials physicochemical properties. Even so, it is still unclear how the physicochemical properties of aspect ratio (AR), surface charge and surface chemistry contribute to GNR cellular association and cytotoxicity. In this report, we showed that surface chemistry is primarily responsible for cytotoxicity and cellular association of GNRs. Results demonstrated that with the removal or sequestration of cetyltrimethylammonium bromide (CTAB) both negatively and positivity charged GNRs had significantly enhanced biocompatibility. In addition, when GNR deposition was accounted for, the materials AR and primary surface charge had minimum overall impacted on cytotoxicity and cellular association of GNRs. These findings identify surface chemistry as primarily responsible for cytotoxicity and cellular association of GNRs, enabling the development of GNRs with enhanced biocompatibility for new nano-based biomedical applications.

15. SUBJECT TERMS

16. SECURITY CLASSIFICATION OF:			17. LIMITATION OF ABSTRACT	18. NUMBER OF PAGES	19a. NAME OF RESPONSIBLE PERSON
a. REPORT	b. ABSTRACT	c. THIS PAGE			19b. TELEPONE NUMBER (*Include area code)*
U	U	U			NA

Standard Form 298 (Rev. 8-98)
Prescribed by ANSI-Std Z39-18

THIS PAGE INTENTIONALLY LEFT BLANK.

TABLE OF CONTENTS

LIST OF FIGURES

LIST OF TABLES

PREFACE

Funding for this project was provided through the Air Force Surgeon General Clinical Investigations Program.

The authors would like to acknowledge the Biomedical Sciences PhD program at wright State University. The authors also wish to thank Dr. David Cool, Dr. Courtney Sulentic, Dr. Nancy Bigley and Dr. Sharmila Mukhopadhyay.

THIS PAGE INTENTIONALLY LEFT BLANK.

1.0 SUMMARY

Gold nanorods (GNRs), due to their unique optical & electronic properties are popular candidates for novel nano-based biomedical applications. Unfortunately, previous studies have reported the potential for GNR cytotoxicity related to the materials physicochemical properties. Even so, it is still unclear how the physicochemical properties of aspect ratio (AR), surface charge and surface chemistry contribute to GNR cellular association and cytotoxicity. In this report, we showed that surface chemistry is primarily responsible for cytotoxicity and cellular association of GNRs. Results demonstrated that with the removal or sequestration of cetyltrimethylammonium bromide (CTAB) both negatively and positivity charged GNRs had significantly enhanced biocompatibility. In addition, when GNR deposition was accounted for, the materials AR and primary surface charge had minimum overall impacted on cytotoxicity and cellular association of GNRs. These findings identify surface chemistry as primarily responsible for cytotoxicity and cellular association of GNRs, enabling the development of GNRs with enhanced biocompatibility for new nano-based biomedical applications.

2.0 INTRODUCTION

Nanomaterials hold the potential to transform an unprecedented range of industries including the medical diagnostics and treatment of diseases (Adlakha-Hutcheon et al., 2009; Barreto et al., 2011). Gold nanorods (GNRs), due to their unique optical properties, have been identified as a strong candidate for many nano-base biomedical applications. The optical properties of GNRs are tunable by changing the aspect ratio (AR) or surface chemistry (Bouhelier et al., 2005). The AR describes the proportional relationship between the nanomaterial's width and its height. Depending on the GNR AR, a narrow range of frequencies of light induce conduction band electron oscillation and this resonance is called the surface plasmon resonance (SPR). For GNRs, it occurs in the visible and near-infrared of the spectrum. GNRs with ARs of approximately 3 and greater have SPRs in the near-infrared range where light has minimal impact on living cells (Huang et al., 2006). In addition, by combining GNRs of differing ARs, and therefore differing near-infrared SPR wavelengths, would enable multiplexing of a multitude of biomedical applications. (Sepúlveda et al., 2009; Wijaya et al., 2009; Yu & Irudayaraj, 2006). These include diagnostic imaging, photo-therapies, and drug/gene delivery (Agarwal et al., 2011; Nagesha et al., 2007; Pandey et al., 2013; Pissuwan et al., 2008). Unfortunately, many studies have reported GNR cytotoxicity preventing the implementation of new GNR-based biomedical applications.

Physicochemical properties (size, shape, aspect ratio, charge and surface chemistry) of GNRs have all been suggested to influence both cellular uptake and cytotoxicity of these materials (Goodman et al., 2004; Grabinski et al., 2011; Schaeublin et al., 2011). Even so, there exists considerable uncertainty as these and previous studies failed to comprehensively control for the physicochemical properties of GNRs.

2.1 Objective

The aim of this study is to determine how GNR AR and surface charge affects GNR cellular association and cytotoxicity, *in vitro*. This will be evaluated by comparing different ARs (approximately 1, 2, and 3) of a negatively charged sets of GNRs to a positively charged sets of GNRs, (Tannic acid (TA) coated cetyltrimethylammonium bromide (CTAB-TA)) GNRs and (11-mercaptoundecyl trimethylammonium bromide (MTAB)) GNRs. It is hypothesized that by manipulating GNR aspect ratio, surface charge and chemistry we can enhance their biocompatibility while maintaining their cellular uptake.

3.0 METHODS

3.1 Synthesis of GNRs

MTAB GNRs (MTAB-1, MTAB-3 and MTAB-3) were purchased from Nanopartz (Loveland, CO, USA). All other GNRs (CTAB, CTAB-TA-1, CTAB-TA-1, CTAB-TA-3, CTAB-TA and PEG) were synthesized according to a modified seed mediated procedure reported by Park and Vaia (2008). Briefly, a seed solution of CTAB (0.1 M) and chlorauric acid (0.1 M) was combined at room temperature with a growth solution of CTAB (0.1 M), chlorauric acid (0.1 M) silver nitrate (0.1 M) ascorbic acid (0.1 M). The CTAB was purchased from GFS chemicals (Powell, OH, USA). The chloroauric acid, ascorbic acid, silver nitrate, sodium borohydride, sodium Chloride, MOPS buffer and tannic acid were obtained from Sigma Aldrich (St Louis, MO, USA).

3.2 PEG functionalization of GNRs

CTAB GNRs were functionalized with PEG as previously reported (Untener et al., 2013) with modifications. Briefly, the GNRs were functionalized overnight with 1 mM thiol PEG (Nanocs, Boston, MA) two times (MW 20000 followed by MW 5000) to displace the surface bound CTAB molecules. The GNR samples were centrifuged at 8,000g and the supernatant was removed and replaced with sterile water to remove residual free CTAB.

3.3 TA functionalization of GNRs

Method 1: was used for the functionalization of CTAB-TA-1, CTAB-TA-2 and CTAB-TA-3 GNRs. CTAB GNRs were functionalized with TA as previously reported (Untener et al., 2013) with modifications. Briefly, the GNRs were functionalized overnight with 1 mM TA three times to overcoat the surface bound CTAB molecules. The GNR samples were centrifuged at 8,000g and the supernatant was removed and replaced with sterile water to remove residual free CTAB and TA.

Method 2: was used for the functionalization of TA-3 GNRs. CTAB GNRs were functionalized with TA according to a modified procedure reported by Ejima et al. (2013) stepwise with TA (24mM), and MOPS buffer (100 mM, pH 7.4) with vortexing after each addition. The GNR samples were then centrifuged at 3,000g and the supernatant was removed and replaced with sterile water to remove residual TA. The MOPS buffer and tannic acid were obtained from Sigma Aldrich (St Louis, MO, USA).

3.4 Characterization of GNRs

GNR characterization was performed to determine their key physicochemical properties and to verify particle uniformity prior to experiments. The purity and spectral signature of the GNRs were analyzed before use with UV−Vis spectrometry on a Bio TEK Synergy HT (Winooski, VT, USA) instrument. For evaluation of rod size and morphology, nanoparticles in solution were placed onto a Formvar carbon coated copper TEM grid (Electron Microscopy Sciences, Hatfield, PA, USA) and dried. They were imaged with transmission electron microscopy (TEM) using a Hitachi H-7600 with an accelerating voltage of 120 kV. To assess the surface charge of the GNRs, zeta potential measurements were taken using laser Doppler electrophoresis on a Malvern Zetasizer, Nano-ZS. Agglomerate sizes of the GNRs in media were determined through dynamic light scattering (DLS), also on a Malvern Zetasizer (Malvern Instruments, MA, USA).

3.5 Cell culture conditions

The A549 human lung, cell line (American Type Culture Collection (ATCC), Manassas, VA, USA) and HepG2 human livercell line (ATCC, Manassas, VA, USA) were maintained in RPMI 1640 cell culture media (Life Technologies, Grand Island, NY, USA) supplemented with 10% fetal bovine serum (Hyclone, Logan, UT, USA) and 1% penicillin streptomycin. Cells were maintained in a humidified incubator controlled at 37 °C and 5% CO_2. The same media composition was used for all GNR exposure procedures.

3.6 Cellular viability assessment

A549 human lung cell viability was evaluated using the CellTiter 96 Aqueous One Solution (MTS) (Promega, Madison, WI, USA) which monitors mitochondrial function and MultiTox-Glo Assay (LCDC) (Promega, Madison, WI, USA), which sequentially measures two protease activities; one is a marker of cell viability, and the other is a marker of cytotoxicity. Cells were seeded into a 96-well plate at a concentration of 2×10^3 cells/well and the following day treated with the stated GNR conditions. After exposure period, the cells viability was determined in accordance with the manufacturer's protocol. Result represents three independent trials with the average ± the standard error reported.

3.7 ROS assay

The intracellular generation of reactive oxygen species (ROS) after GNR exposure was evaluated using CM-H2DCFDA (Life Technologies, Grand Island, NY, USA) Technologies, Grand Island, NY) which is based on intracellular esterases and oxidation that yields a fluorescent product that is trapped inside the cell. Cells were seeded into a 96-well plate at a concentration of 2×10^3 cells per well and the following day treated with the stated GNR conditions. After 1 h, 6 h, and 24 h the intracellular ROS generation was determined in accordance with the manufacturer's protocol. Result represents three independent trials with the average ± the standard error reported.

3.8 Quantification of cellular uptake of GNRs by ICP-MS

A total of 1×10^5 cells/well were seeded on 12mm diameter glass slides in a 24-well plate and dosed with 5 μg/mL GNRs for 24 h. The cell samples were then washed three times with warm PBS (with the exception of the deposition study samples) and digested with an aqueous solution containing 0.05% Triton X-100, 3% HCl, and 1% HNO_3. The intracellular gold concentration was determined through inductively coupled plasma mass spectrometry (ICP-MS) on a Perkin-Elmer ICP-MS 300D instrument (Santa Clara, CA). ICP-MS was conducted in standard mode with 20 sweeps per reading, at one reading per replicate, and three replicates per sample with a dwell time of 100 ms. A calibration curve was obtained using four gold standard solutions and the addition of an internal standard was done to ensure that no interferences were occurring. Results represented three independent trials with the average ± the standard error reported.

3.9 Brightfield and darkfield microscopy

A549 human lung cells were seeded at 1.25×10^5 cells per chamber on a 2-well chambered slide and grown for 24 h. The following day the cells were dosed with 10 μg/mL GNRs for 24 h. After 24 h, the cells were fixed with 4% paraformaldehyde and incubated with Alexa Fluor 555-phalloidin for actin staining and DAPI for nuclear staining (Life Technologies, Grand Island,

NY). The slides were then sealed and imaged using a CytoViva 150 ultra resolution attachment on an Olympus BX41 microscope (Aetos Technologies, Opelika, AL). All experiments were performed at minimum three times. Care was taken to ensure full evaluation of each slide for well represented images.

3.10 Transmission electron microscopy

A549 human lung cells were seeded in a 6-well plate at 6×10^5 cells/well for 24 h then exposed to the stated GNRs concentration (5 and 20 μg/mL) and washed three times with warm PBS. The cells then fixed overnight in 2% paraformaldehyde and 2% glutaraldehyde after indicated duration (24 h, 4 days or 8 days). The cells were then stained with 1% osmium tetroxide, washed, and subsequently dehydrated with ethanol dilutions ranging from 50 to 100%. The cells were then embedded in LR White resin and cured overnight at 60 °C under a vacuum, after which the samples were sectioned using a Leica EM UC7 Ultramicrotome. Cell sections of 70 nm in thickness were placed on a Formvar carbon coated copper TEM grid (Electron Microscopy Sciences, Hatfield, PA) and were imaged. Transmission electron microscopy (TEM) was performed using a Hitachi H-7600 with an accelerating voltage of 120kV. All experiments were performed at minimum three times. Care was taken to ensure full evaluation of each sectioned sample for well represented images.

3.11 Statistical analysis

All experimental results represent a minimum of three independent trials unless otherwise stated. Data are expressed as the mean ± the standard error of the mean (SEM). Statistical calculations were performed using SAS (Version 9.1) or GraphPad Prism (version 5.02, GraphPad Software Inc. La Jolla, CA, USA) to determine statistical significance at p values of <0.05 (*), <0.01 (**) , or <0.001 (***).

4.0 RESULTS AND DISCUSSION

4.1 GNR characterization

GNR characterization was performed to determine their key physicochemical properties and to verify particle uniformity prior to experiments. ARs of 1, 2, and 3 were selected to determine the role of AR on cytotoxicity and cellular association/uptake in study. The GNRs had a diameter of 23 ± 0.76 nm on average, with the exception for the AR 1 CTAB TA coated GNRs (CTAB-TA-1) that had a diameter of 9 ± 0.9 nm. AR 2 GNRs had a length of 48 ± 1.0 nm on average and AR 3 GNRs had a length of 65 ± 4.0 nm on average. TEM images demonstrated that GNR sets were uniform in size and morphology (Figure 1 and Table 1). UV−Vis analysis confirmed predicted SPR peaks based on calculated AR (Figure 1J) (Jun et al., 2008). AR 3 GNRs had an average SPR peak of 700.3 ± 5.0, nm which falls in the NIR “water window” region, making the GNRs candidates for biomedical applications. To determine GNR surface charge, zeta potential analysis was performed on each particle (Table 1). Zeta potential analysis measures the velocity a charged GNRs move in a voltage field and can be quantified by tracking the GNRs as they migrate in the voltage field. From this analysis, it was shown that both CTAB and MTAB GNRs were positively charged as expected due to the quaternary ammonium cation. PEG GNRs exhibited a neutral charge, while CTAB-TA GNRs displayed a negative surface charge,

confirming that functionalization with PEG or TA was successful. Dynamic light scattering was used to determine hydrodynamic size of GNR groupings after exposure to a protein rich environment (culture media). Hydrodynamic size of GNRs in media showed that TA coated GNRs were on average larger than the MTAB GNRs of the same AR.

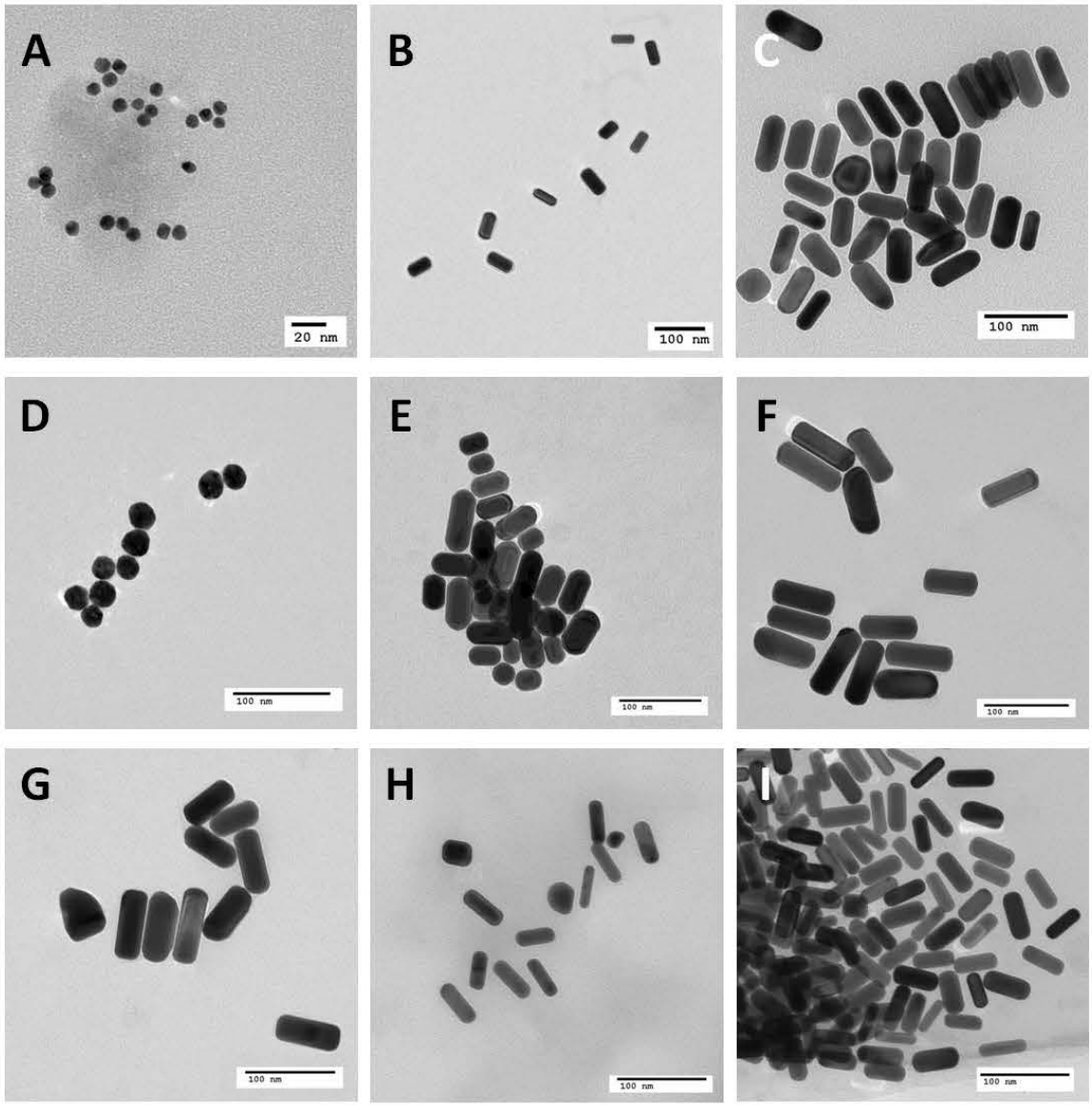

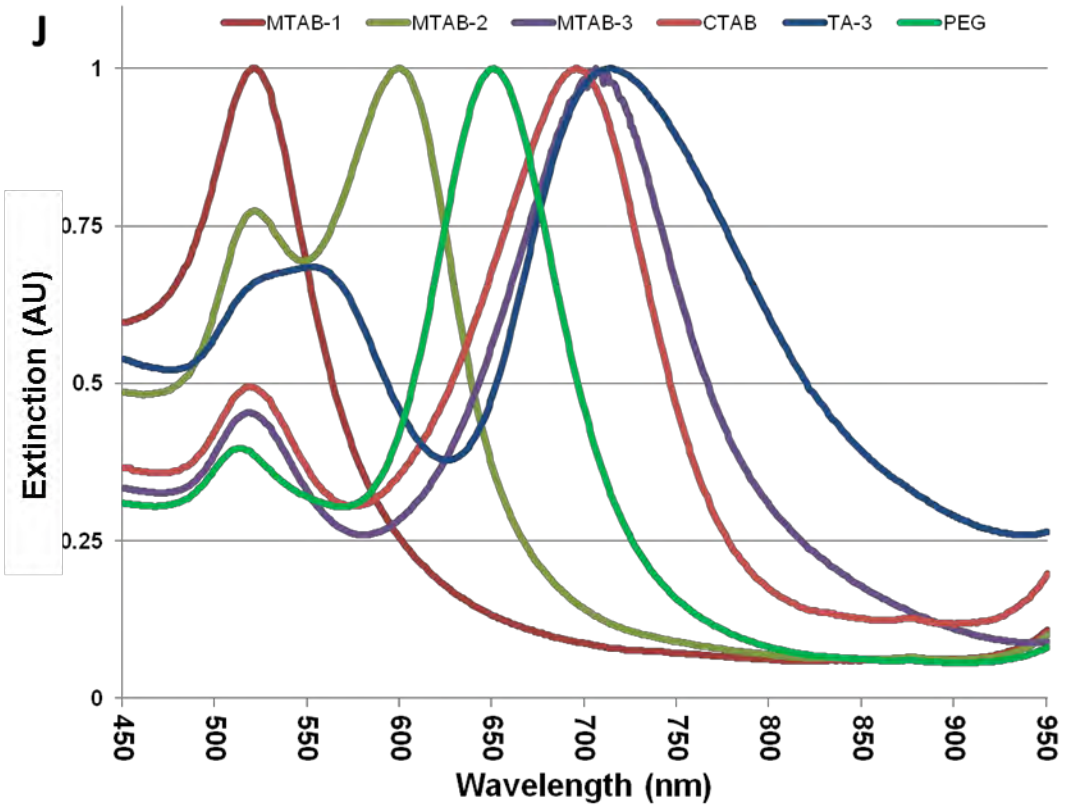

Figure 1. GNR characterization.
Representative TEM images of Representative TEM images A. CTAB-TA-1, B. CTAB-TA-2 C. CTAB-TA-3 D. MTAB-1 E. MTAB-2 F. MTAB-3 G. CTAB H. CTAB-TA I. PEG; J. UV-Vis absorption spectra of MTAB-1 (dark red), MTAB-2 (dark green), MTAB-3 (purple), CTAB (red), TA-3 (blue) and PEG (light green) GNRs.

Table 1. Characterization of GNRs

Name	Primary Size (nm)	Aspect Raito	Surface Chemistry	Surface Charge (mV)	Hydrodynamic Diameter in Media (nm)
CTAB-TA-1	9x9 ±0.9	1	CTAB-TA	-23.4	93.7 ±1.8
CTAB-TA-2	23x49 ±4.9	2.2	CTAB-TA	-31.4	116.0 ±4.1
CTAB-TA-3	23x62 ±6.8	2.7	CTAB-TA	-26.0	653.0 ±68.9

MTAB-1	25x25 ±1.5	1	MTAB	25.1	117.4 ±1.1
MTAB-2	25x47 ±5.4	1.9	MTAB	35.2	124.3 ±6.4
MTAB-3	25x73 ±2.7	2.9	MTAB	32.8	182.3 ±3.7
CTAB	25x72 ±3.1	2.9	CTAB	37.2	318.7 ±4.3
TA-3	22x60 ±2.1	2.8	CTAB-TA	-19.4	416.4 ±35.2
PEG	19x48 ±2.6	2.5	PEG	2.1	75.2 ±0.9

4.2 Cellular association of negatively charged GNRs of differing ARs

Visualization of cellular morphology and association of CTAB-TA GNRs of differing ARs were examined using brightfield, darkfield and TEM microscopy (Figure 2, 3 and 4). After 24 h exposure to the GNRs (5 μg/mL), the cells were assisted by brightfield microscopy. CTAB-TA-1 and CTAB-TA-2 exposed cells showed no change in appearance when compared to control cells. However, CTAB-TA-3 exposed cells no longer appear confluent with possible changes in cellular morphology (Figure 2). To confirm any changes in cellular morphology and to examine GNR cellular association, darkfield microscopy was performed. Results demonstrated that CTAB-TA GNRs of all ARs interacted with A549 cells and had a high level of cellular association. In addition, darkfield images revealed both CTAB-TA-2 and CTAB-TA-3 exposed cells displayed altered cellular morphology compared to control cells (Figure 3). Finally, TEM microscopy was performed to examine GNR internalization and further observe any changes in cellular morphology. TEM images showed the presence of internalized negatively charged GNRs of all ARs (Figure 4). However, the GNRs with an AR greater than 2 displayed altered cellular morphology. CTAB-TA-2 exposed cells show vacuoles with a ribbon like structure, possibly lamellar bodies (Figure 4B). Alterations in lamellar bodies in A549 human lung epithelial cells have been reported as an indication of pre-cytotoxicity (Davoren et al., 2007). In addition, CTAB-TA-3 exposed cells displayed extremely large vacuoles with a small number of GNRs seen in the cells and a majority of the GNRs around the cells (Figure 4C and black arrow). These changes in cellular morphology could be an indication of cytotoxicity. Therefore, an assessment of cellular viability was performed.

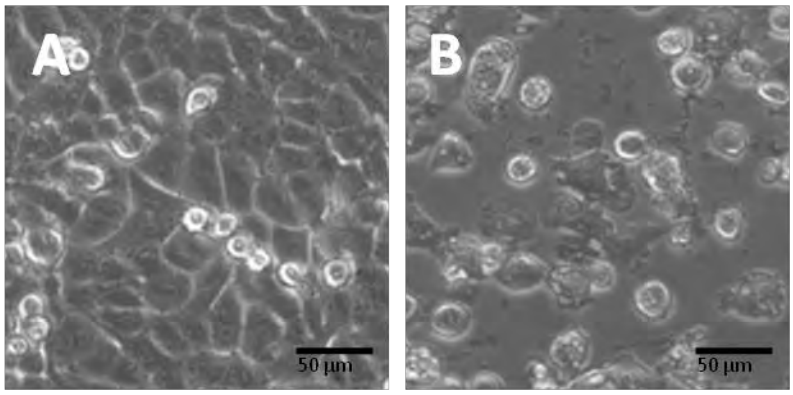

Figure 2. Negatively charged CTAB-TA GNRs AR3 alter A549 cells.

Representative brightfield images following CTAB-TA-3 GNR (5 µg/mL) exposure. A. Control, B. CTAB-3 GNRs. Results illustrate CTAB-TA-3 exposed cells no longer appear confluent with possible changes in cellular morphology.

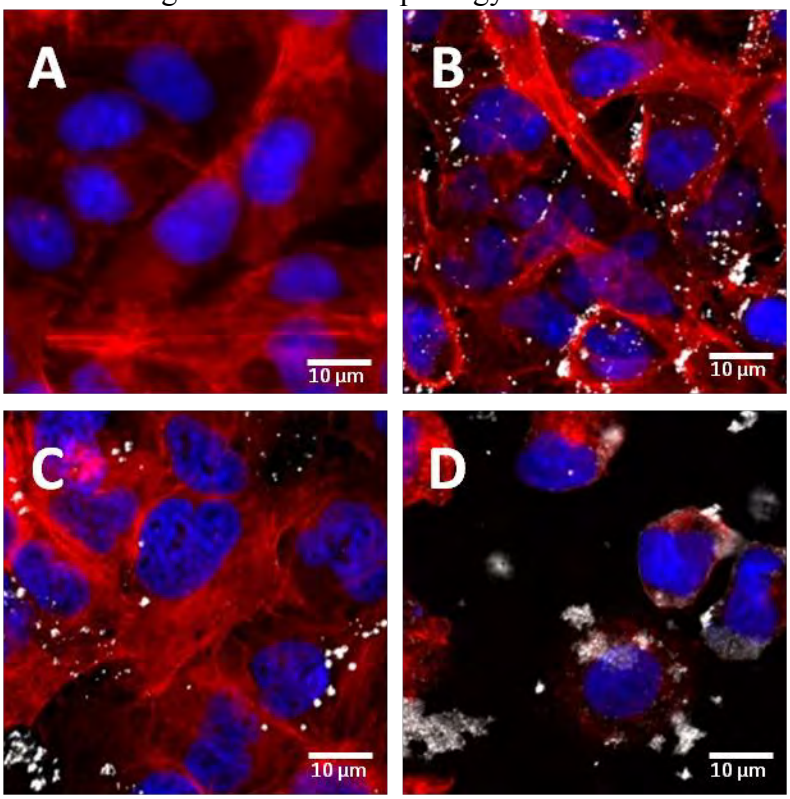

Figure 3. Higher AR CTAB-TA GNRs alter A549 morphology.
Representative Darkfield Images. Fluorescent images following GNR exposure (5 µg/mL) of differing AR A. Control, B. CTAB-TA-1, C. CTAB-TA-2 and C. CTAB-TA-3. Fluorescent images results illustrate the cellular association of GNMs and the morphology of A549 cells. CTAB-TA-1 exposure showed no apparent change in morphology of A549 cells. However, both CTAB-TA-2 and CTAB-TA-3 displayed altered cellular morphology. A549 cells underwent actin (red) and nuclear (blue) staining with GNRs (reflecting white).

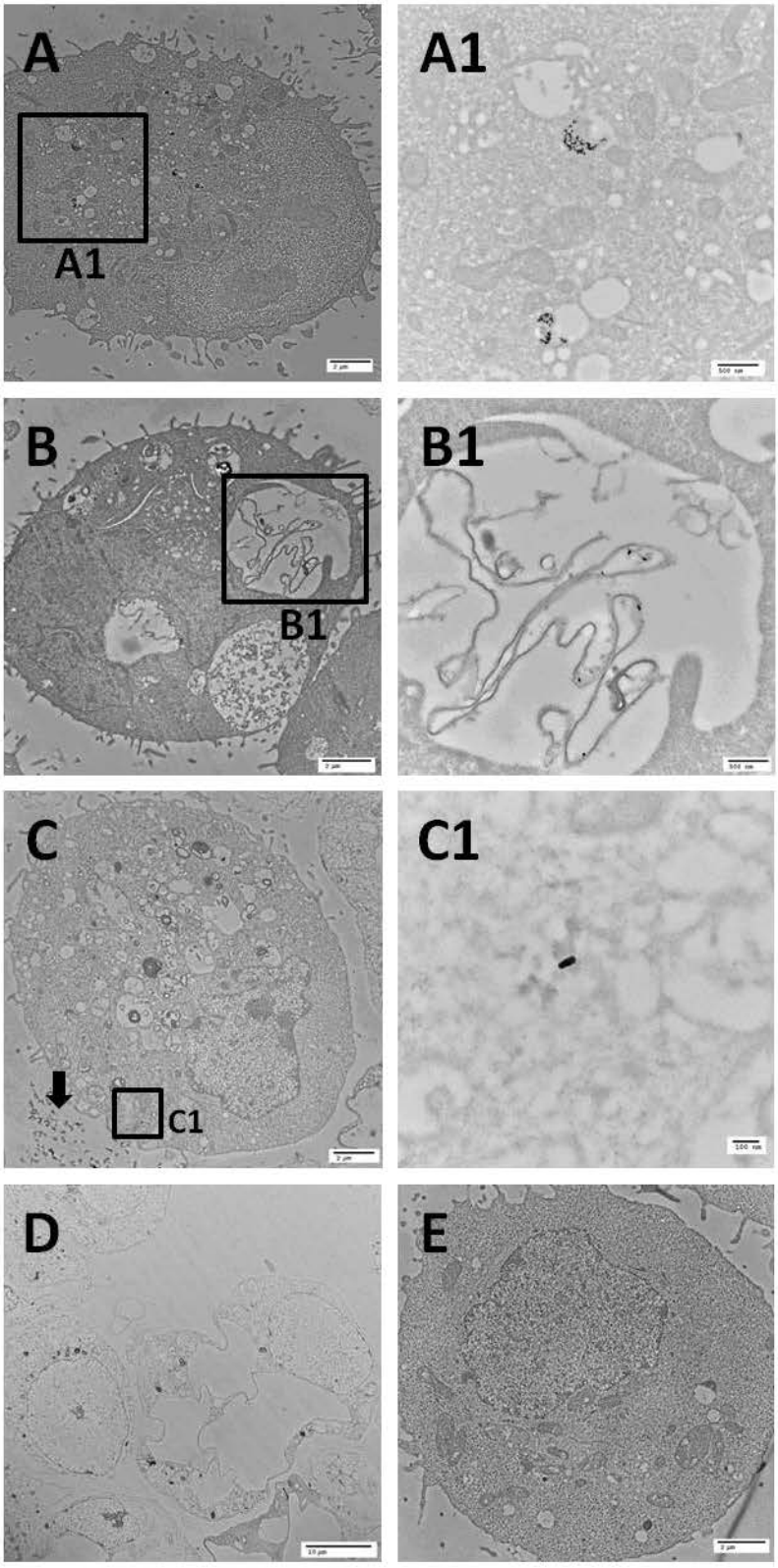

Figure 4. Negatively charged CTAB-TA GNRs are internalized by A549 cells.

Representative TEM images of A549 cells after exposure to negatively charged GNRs (5μg/ml) for 24h. A. CTAB-TA-1 B. CTAB-TA-2 C-D. CTAB-TA-3 E. Control. Results demonstrated the presences of internalized negatively charged GNRs of all ARs (1-3). However, A549 cells display altered morphology after exposure to CTAB-TA-2 and CTAB-TA-3 GNRs compared to control.

4.3 Cytotoxicity of negatively charged GNRs of differing ARs

A549, human lung cells were exposed to GNRs (10 μg/mL) for 24 h. Membrane integrity and mitochondrial function was determined to assess the cytotoxicity of the negatively charged GNRs of differing ARs. Cells that were exposed to CTAB-TA-3 GNRs showed a significant decrease in cell viability (Figure 5) and concentration dependent cytotoxicity. As all GNRs tested have a negative surface charge, the demonstrated cytotoxicity of the CTAB-TA-3 GNRs may be due to their higher AR or surface chemistry. To test these possibilities, the cytotoxicity of positively charged GNRs of differing ARs was examined.

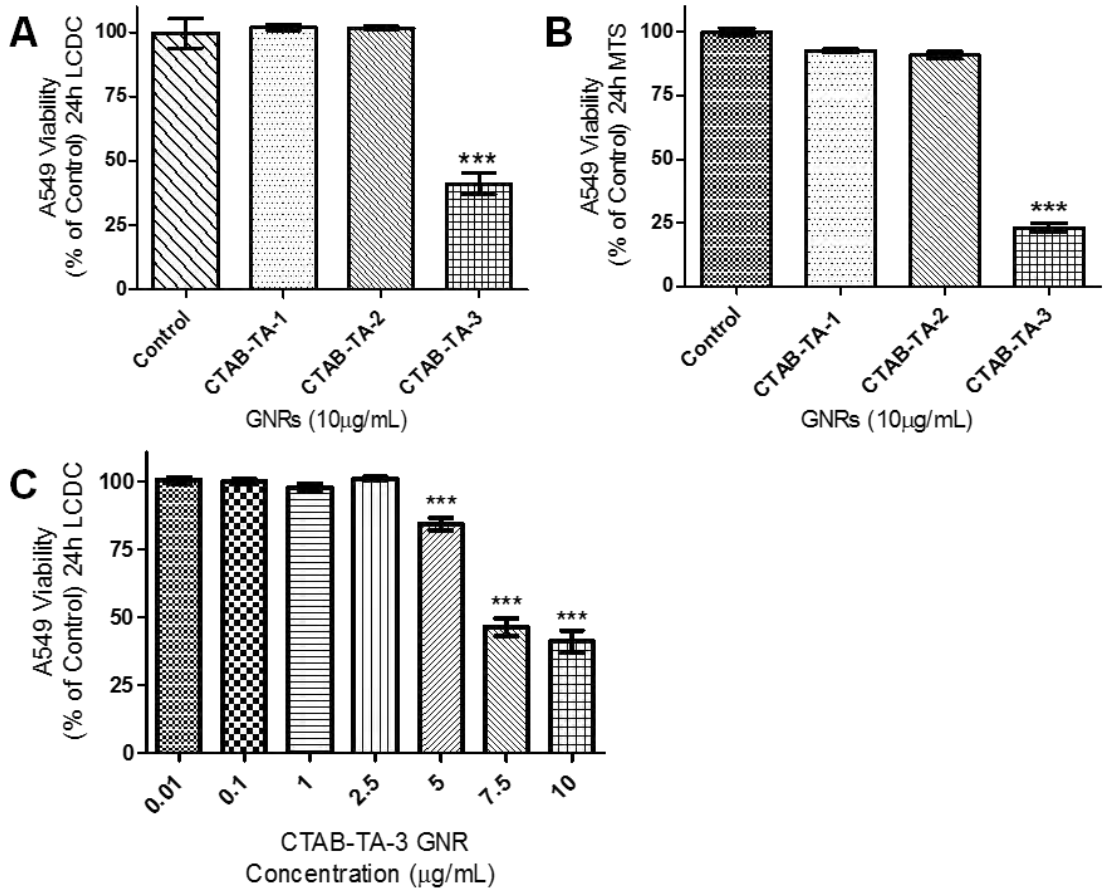

Figure 5. Cytotoxicity of negatively charged higher AR GNRs.

A549 human lung cells were exposed to negatively charged CTAB-TA GNRs of differing ARs (up to 10 μg/mL) for 24 h, cell viability was assessed using A. LCDC and B. MTS assays and represented relative to the control cells. C. Results showed CTAB-TA-3 GNRs significantly decrease cell viability after exposure to concentrations as low as 5 μg/mL. Statistical significance was determined using a one way ANOVA with Dunnett's post-hoc tests.

4.4 Biocompatibility of positively charged GNRs of differing ARs

A549 human lung cells were exposed to GNRs (10 μg/mL or 20 μg/mL) for 24 h. Next, membrane integrity and mitochondrial function was determined to assess the cytotoxicity of the positively charged GNRs of differing ARs. After exposure to MTAB GNRs (10 μg/mL), A549 cells showed no significant effects on their cellular viability (Figure 6A-B).

To confirm that MTAB GNRs enhanced biocompatibility, they were evaluated with a second cell line, HepG2 human liver cells. After exposure to MTAB GNRs (10 μg/mL), HepG2 cells also showed no significant decrease of cellular viability (Figure 7A-B). Finally, A549 cells were exposed to MTAB GNRs at four-times the cytotoxicity concentration of CTAB-TA-3 GNRs (20 μg/mL). This again resulted in no significant decrease of cellular viability (Figure 8).

Next, cellular stress was examined by measuring changes in reactive oxygen species (ROS) after cellular exposure to the GNRs as this has been reported as an indicator of GNR biocompatibility (Wang et al., 2011). The 6 h time point was chosen based on maximum ROS response before cell death. A549 and HepG2 cells showed no significant increase in ROS levels after exposure to MTAB GNRs (Figure 6C and 7C).

One possible explanation of the differences in cytotoxicity may be due to differences in GNR cellular association and/or uptake. To check these possibilities,MTAB GNR cellular association by TEM and uptake by Inductively Coupled Plasma Mass Spectrometry (ICP-MS) was tested.

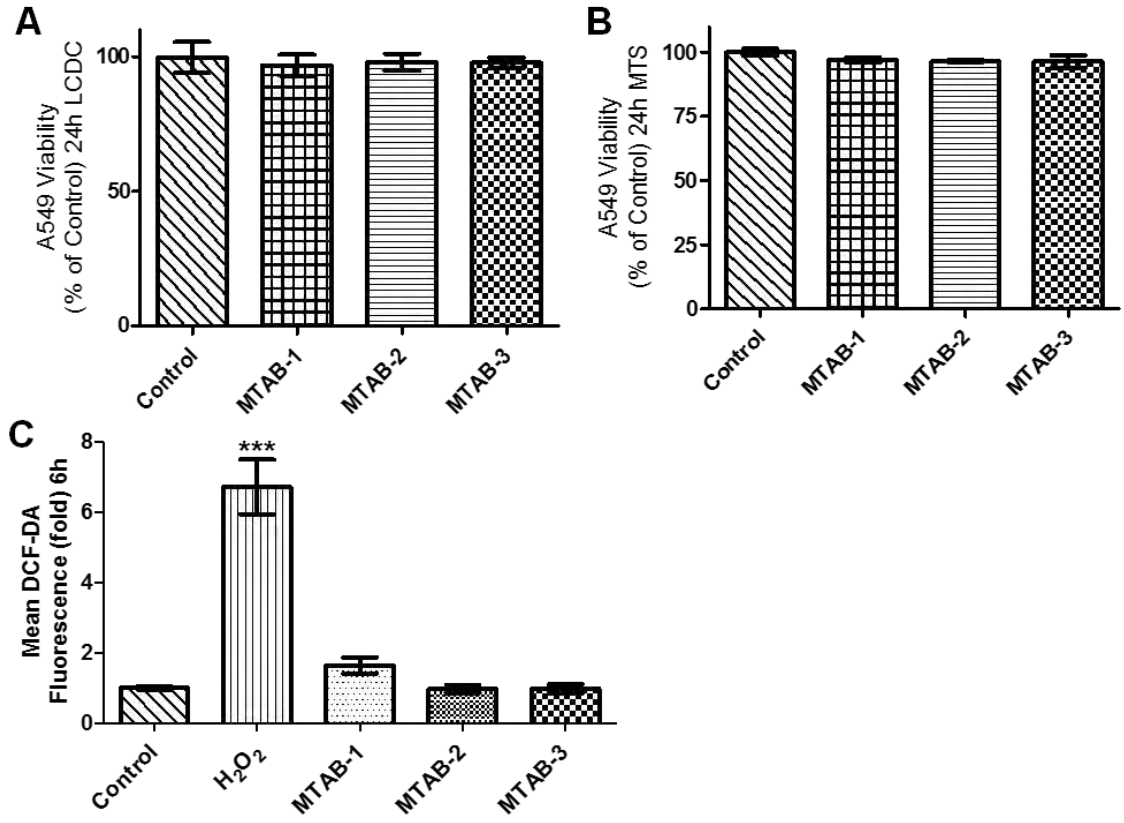

Figure 6. Positively charged MTAB GNRs do not decrease A549 cell viability.

A549 human lung cells were exposed to positively charged MTAB GNRs of differing ARs (10 μg/mL) for 24 h, cell viability was assessed using A. LCDC and B. MTS assays and represented relative to the control cells. Results showed MTAB GNRs do not significantly decrease cell viability. C. ROS assay demonstrated no significant increase in ROS after exposure to MTAB GNRs. Statistical significance was determined using a one way ANOVA with Dunnett's post-hoc tests.

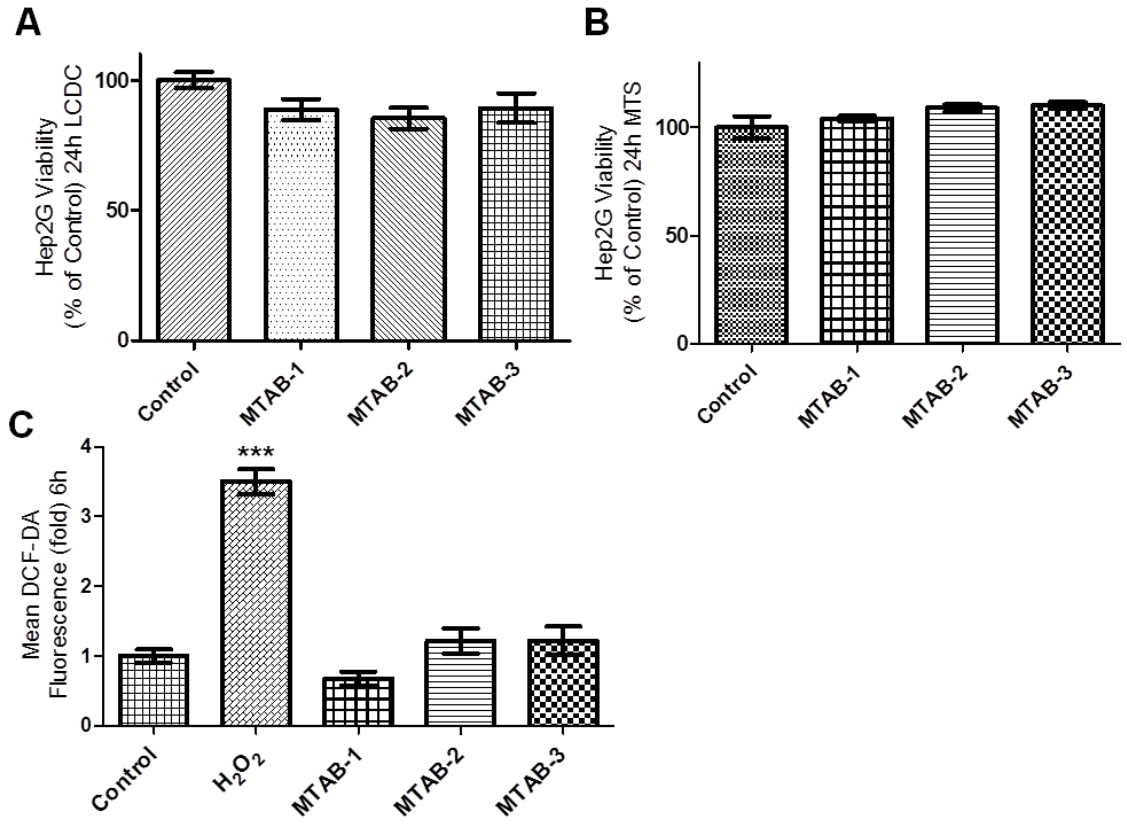

Figure 7. Positively charged MTAB GNRs do not decrease HepG2 cell viability. HepG2 human liver cells were exposed to positively charged MTAB GNRs of differing ARs (10 μg/mL) for 24 h, cell viability was assessed using A. LCDC and B. MTS assays and represented relative to the control cells. Results showed MTAB GNRs do not significantly decrease cell viability. C. ROS assay demonstrate no significant increase in ROS after exposure to MTAB GNRs. Statistical significance was determined using a one way ANOVA with Dunnett's post-hoc tests.

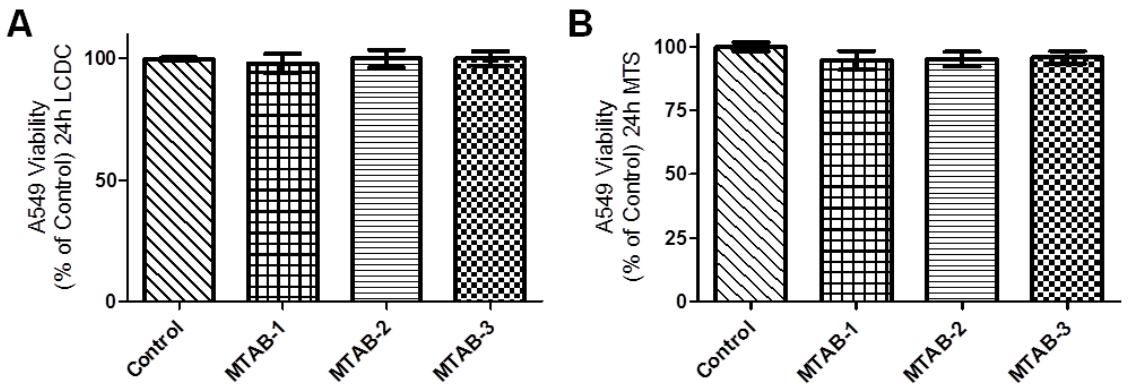

Figure 8. Biocompatibility of positively charged MTAB GNRs.
A549 human lung cell were exposed to MTAB GNRs at 4 times the cytotoxic concentration of CTAB-TA-3 GNRs (20 μg/mL) for 24 h, cell viability was assessed using A. LCDC and B. MTS assays and represented relative to the control cells. Results showed MTAB GNRs do not significantly decrease cell viability regardless of AR. Statistical significance was determined using a one way ANOVA with Dunnett's post-hoc tests.

4.5 Cellular association of positively charged GNRs of differing ARs

TEM was used to verify the presence of MTAB GNRs (5 μg/ml) within the A549 cells after 24 h exposure. Results demonstrated the presence of the positively charged GNRs in the cells regardless of their AR (Figure 9).
Quantification of cellular uptake of the MTAB GNRs (5 μg/ml) of differing AR in A549 and HepG2 cells was determined by ICP-MS. Results indicated that as GNR AR increased, so did cellular uptake. In both A549 and HepG2 cells MTAB-1 had the lowest uptake (3% and 2% of treatment, respectively). MTAB-2 and MTAB-3 reported higher uptake in HepG2 cells (45% and 57% of treatment, respectively) compared to A549 cells (30% in A549 and 29% of treatment respectively). However, when the differences in GNR deposition were accounted for, the difference in % uptake was greatly reduced in both cell lines (Figure 10C-D). These findings indicated that differences in GNR deposition may have a greater impact on cellular uptake than their AR and is in agreement with the findings that sedimentation rates and diffusion effects cellular uptake of GNMs (Cho et al., 2011).
Results showed that the MTAB GNRs are being taken up by A549 and HepG2 cells. This indicated that the lack of GNR uptake was not the reason for the absence of cytotoxicity of higher AR MTAB GNRs. This further suggests that the AR of the GNR is not the cause of the cytotoxicity. Another possible explanation could be due to differences in surface chemistry. To determine the cause of the cytotoxicity in the CTAB-TA-3 GNRs, the toxicity of free CTAB and TA was evaluated. Finally, the biocompatibility of GNRs of approximately the same AR (~AR3) with differing surface chemistries was evaluated.

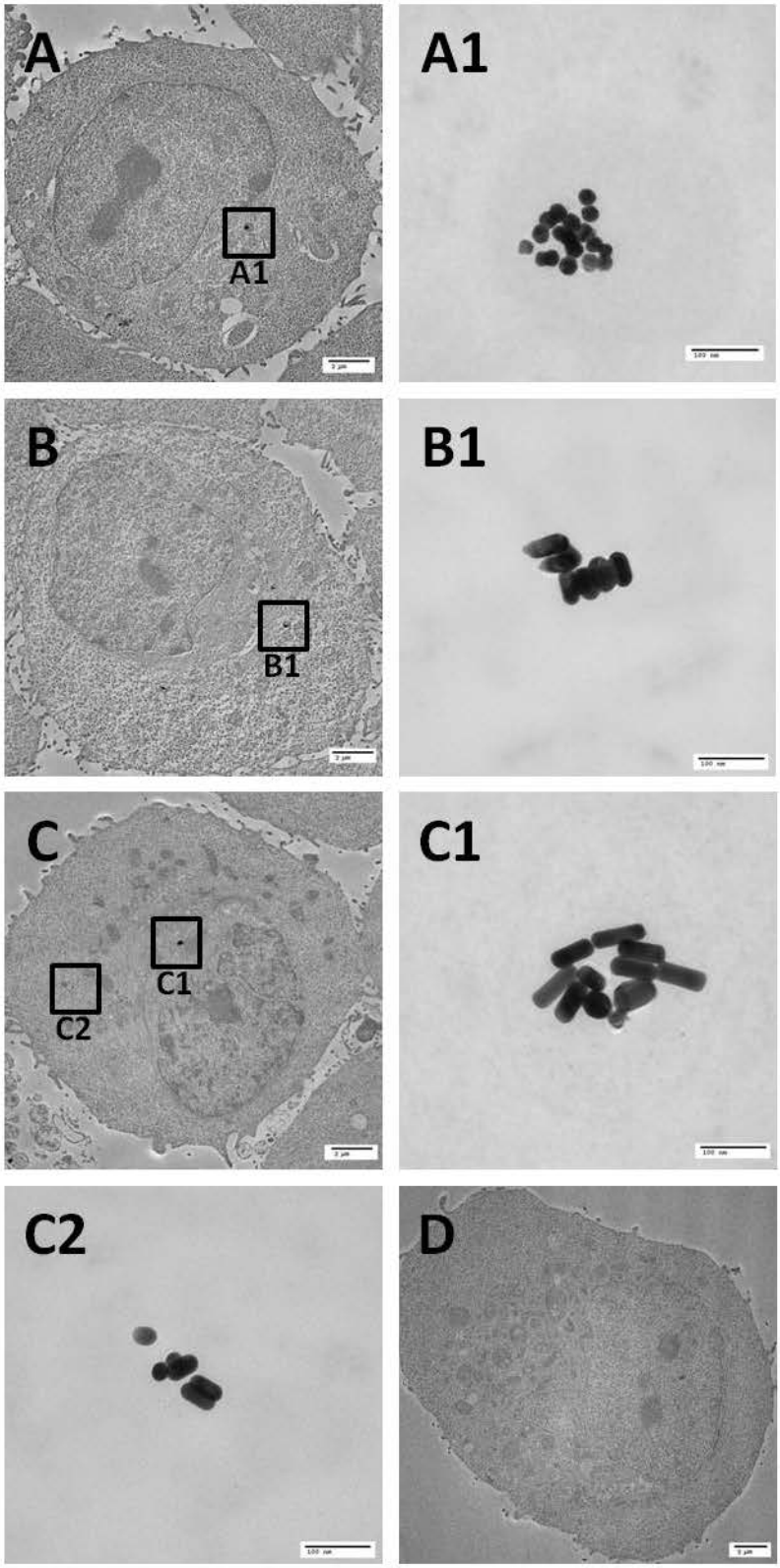

Figure 9. Positively charged MTAB GNRs are internalized by A549 cells.
Representative TEM images of A549 cells after exposure positively charged GNRs (5µg/ml) for 24h. A. MTAB-1 B. MTAB-2 C. MTAB-3 D. Control. Results demonstrated the presence of

internalized positively charged GNRs of all ARs (1-3), suggesting MTAB GNRs were taken up by A549 cells.

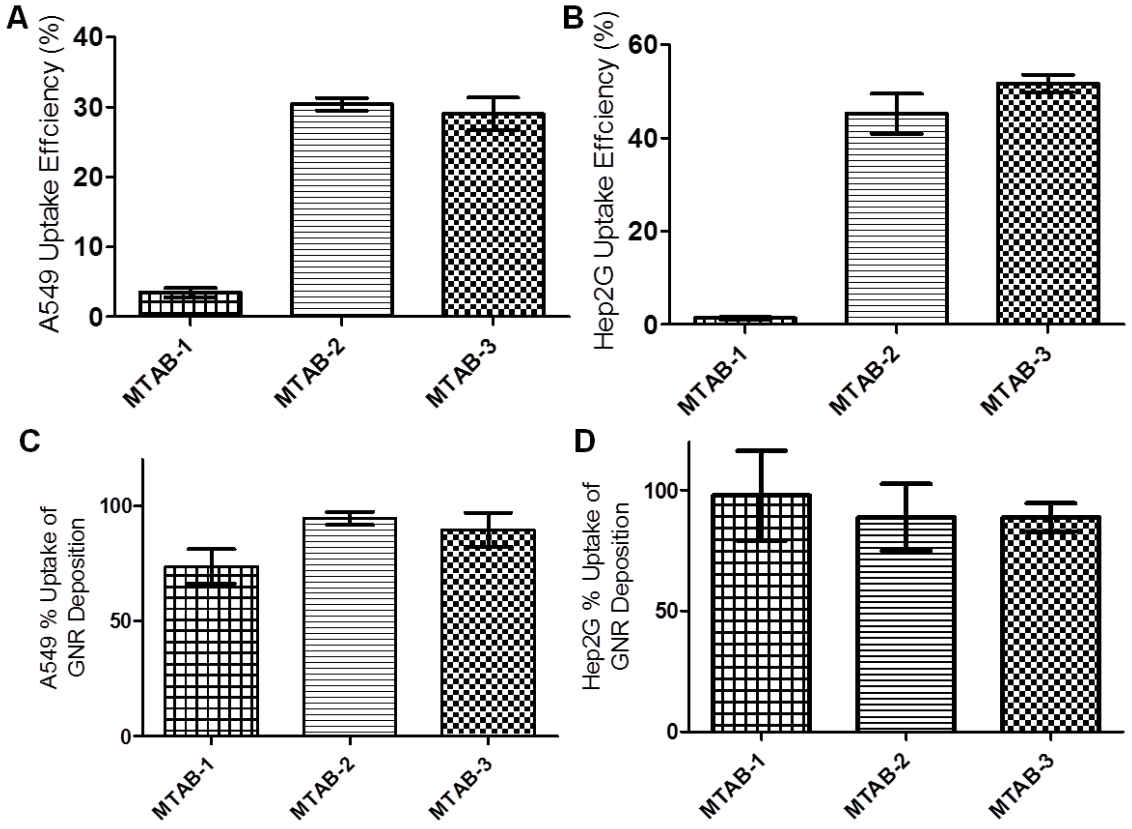

Figure 10. Quantification of cellular uptake of positively charged GNRs.
A549 human lung cells were exposed to positively charged MTAB of differing ARs (5 μg/mL) for 24 h, GNR uptake was quantified using ICP-MS. A. Uptake in A549 cells were 3% (MTAB-1), 30% (MTAB-2) and 29% (MTAB-3) of treatment, respectively. B. Uptake in HepG2 cells were 2% (MTAB-1), 45% (MTAB-2) and 57% (MTAB-3) of treatment, respectively. Results indicated on average that the higher the AR, the more GNRs were present in the cells. However, when the differences in GNR deposition was accounted for, the difference in % uptake was greatly reduced in both cell lines C. A549 cells 74% (MTAB-1), 95% (MTAB-2) and 90% (MTAB-3) D. HepG2 cells 98% (MTAB-1), 89% (MTAB-2) and 89% (MTAB-3). Statistical significance was determined using a one-way ANOVA with a Tukey post-hoc tests.

4.6 Evaluation of cytotoxicity related to GNR surface chemistry

To determine the cause of the cytotoxicity seen in the CTAB-TA GNRs with higher ARs, the cytotoxicity of free CTAB and TA was tested (Figure 11). Results indicated that free TA only demonstrated a decrease in viability at concentrations above 0.1 mg/mL, which is greater than the amount of TA present with CTAB-TA GNRs. In contrast, free CTAB significantly decreased A549 viability at concentrations as low as 1 μg/mL. MTAB GNRs do not have a CTAB present on their surface as the CTAB-TA GNRs do. As the AR of the CTAB-TA GNR increases so does the amount of CTAB present on the surface of the GNRs. Results indicated that the primary cause of the cytotoxicity seen in the CTAB-TA GNRs of higher AR may have been caused by

leaking of CTAB from the GNRs. Therefore, it may be possible to reduce or eliminate the cytotoxicity seen in the higher AR CTAB-TA GNRs with optimization of TA overcoating to more completely sequester the CTAB. To test this supposition, CTAB GNRs were functionalized with TA according to a modified procedure reported by Ejima et al. (2013). This modified TA functionalization procedure resulted in greater stability of the TA overcoating by raising and stabilizing the pH of the suspension. This is because at a pH of 5 or less the TA overcoating can disassemble allowing the release of CTAB (Ejima et al., 2013).

To evaluate the biocompatibility of the new TA-3 GNRs, membrane integrity and mitochondrial function using A549 human lug cells were evaluated. In addition, these results were compared to other GNRs with ARs of approximately 3 with differing surface chemistries (CTAB, PEG, CTAB-TA-3, and MTAB-3). Results demonstrated that the new functionalization procedure enhanced the biocompatibility of the TA coated CTAB GNRs (TA-3;Figure 12). In addition, results show the higher AR positively charged GNRs (MTAB-3), neutral GNRs (PEG) and negatively charged GNRs (TA-3) all showed no decrease in cell viability. In contrast, both positively charged CTAB GNRs (CTAB) and negatively charged CTAB-TA-3 displayed significant cytotoxicity. Results demonstrated that cytotoxicity was not mediated by surface charge or AR. Instead, these findings further indicated that surface chemistry was the primary driver of cytotoxicity and that controlling and reducing or eliminating CTAB was critical for biocompatibility.

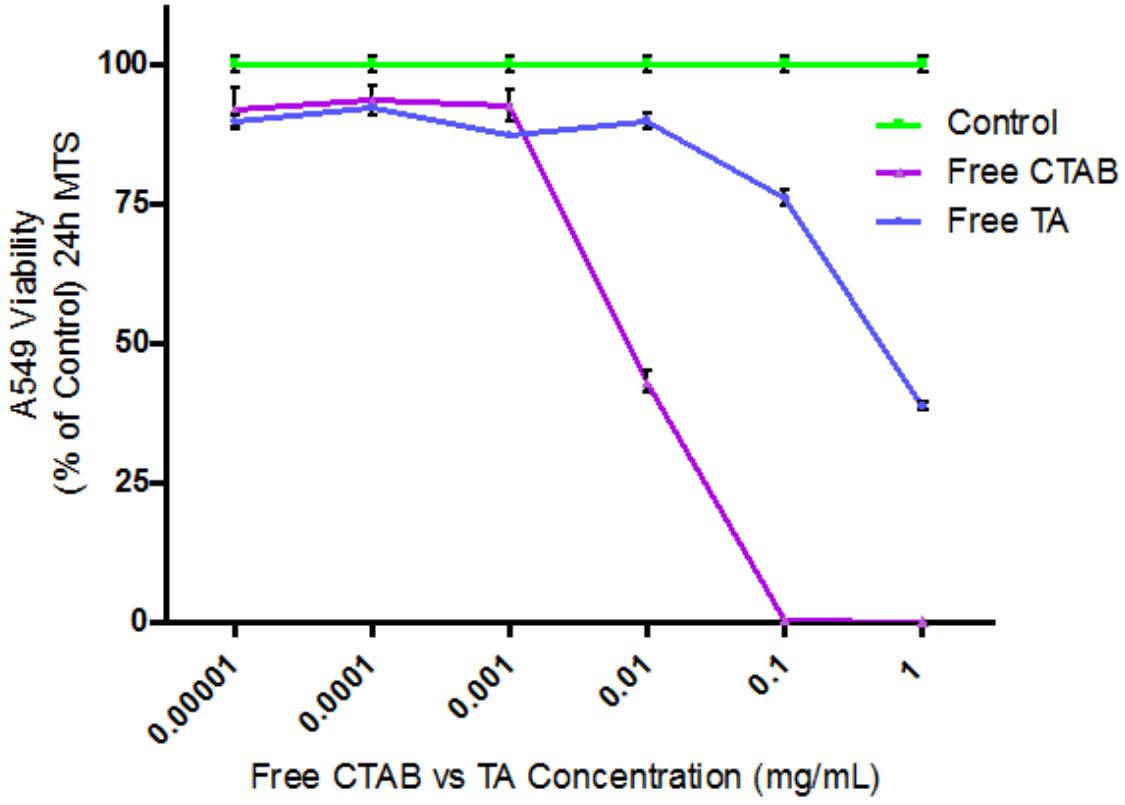

Figure 11. Cytotoxicity of free CTAB and TA.
A549 human lung cells were exposed to increasing concentrations of CTAB and TA (0.00001, 0.0001, 0.001, 0.01, 0.1, 1 μm/mL) in the complete absence of GNRs for 24 h, cell viability was assessed using MTS assay. Free TA only demonstrated a decrease in A549 viability at

concentrations greater than 0.1 mg/mL. Free CTAB significantly decreased in A549 viability at concentrations as low as 1 µg/ml. Results indicated that the primary cause of the cytotoxicity observed with higher AR CTAB-TA GNRs may have been caused by leaking of CTAB from the GNRs.

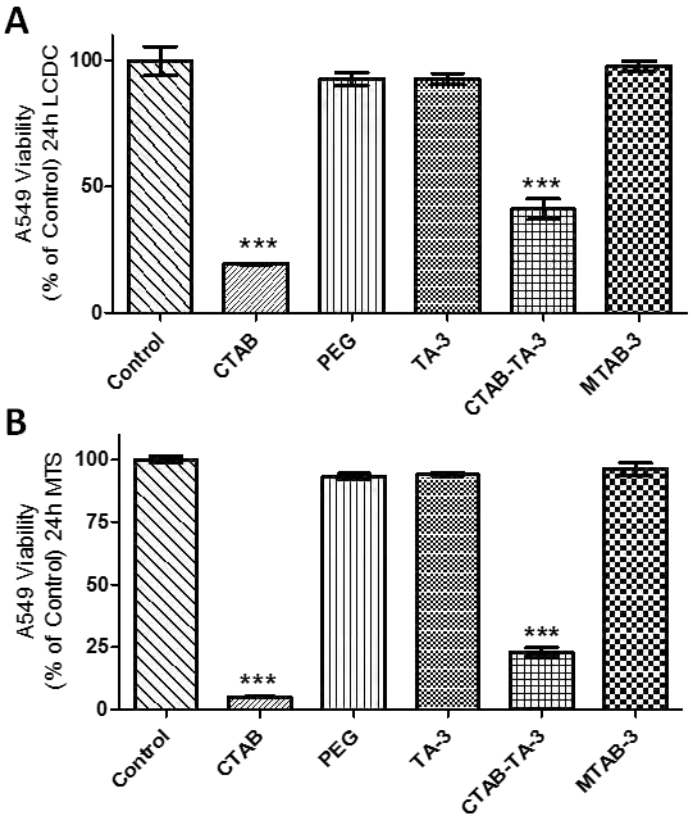

Figure 12. Surface chemistry is responsible for cytotoxicity of GNRs.
A549 cells were exposed to GNRs (10 µg/mL) ~AR3 with differing surface chemistries for 24 h, cell viability was assessed using A. LCDC B. MTS assays results demonstrated the enhanced biocompatibility of the new TA coated GNRs (TA-3). In addition, results showed that the higher AR positively charged GNRs (MTAB-3), neutral GNRs (PEG) and negatively charged GNRs (TA-3) all show no decrease in cell viability. Statistical significance was determined using a one way ANOVA with Dunnett's post-hoc tests.

5.0 CONCLUSIONS

In this study, negatively and positivity charged GNRs of differing ARs were used to determine if they contributed to the cellular association and cytotoxicity of GNRs, *in vitro*. Results demonstrated that the removal or sequestration of CTAB significantly enhanced biocompatibility of the GNRs regardless of their surface charge. In addition, when GNR deposition was accounted for, the material's AR and primary surface charge had minimum overall impact on cytotoxicity and cellular association of GNRs. These results are in agreement with the recently published

work by Wan et al. (2015) that also concluded that surface chemistry, not AR, mediates the biological toxicity of GNRs. In their work they evaluated four ARs (1-4) of bare CTAB GNRs and concluded that because the bare CTAB (AR 1-4) were all cytotoxic, AR does not mediate biological toxicity. However, in order for bare CTAB GNRs to be stable (not aggregate), the concentration of free CTAB has to be higher than the critical micelle concentration. The critical micelle concentration of CTAB is 1 mM (365.45 1 µg/mL) when in water and at 25°C (Fuguet et al., 2005; Quirion & Magid, 1986). In their study, they failed to use a supernatant control to evaluate the cytotoxicity of the free CTAB in the GNR suspension. The cytotoxic concentration of free CTAB was found to be as low as 1 µg/mL (Figure 11) and therefore, the cytotoxicity observed in their study was most likely due to free CTAB. This work demonstrated AR iwas not the main cause of GNR induced cytotoxicity by demonstrating the biocompatibility of three ARs (1-3) of MTAB GNRs in two cell lines.

In conclusion, this study has determined that a GNRs AR and primary surface charge had minimum overall impact on cytotoxicity and cellular association of GNRs, and finds that surface chemistry was the primary driver of cytotoxicity and that controlling and reducing or eliminating CTAB is critical for biocompatibility of GNRs. These findings pave the way for the development of GNRs with enhanced biocompatibility for nano-based bio-medical applications.

6.0 REFERENCES

Adlakha-Hutcheon, G., Khaydarov, R., Korenstein, R., Varma, R., Vaseashta, A., Stamm, H., & Abdel-Mottaleb, M. (2009). Nanomaterials, Nanotechnology. In I. Linkov & J. Steevens (Eds.), Nanomaterials: Risks and Benefits (pp. 195-207): Springer Netherlands.

Agarwal, A., Mackey, M. A., El-Sayed, M. A., & Bellamkonda, R. V. (2011). Remote triggered release of doxorubicin in tumors by synergistic application of thermosensitive liposomes and gold nanorods. ACS Nano, 5(6), 4919-4926. doi: 10.1021/nn201010q

Barreto, J. A., O'Malley, W., Kubeil, M., Graham, B., Stephan, H., & Spiccia, L. (2011). Nanomaterials: applications in cancer imaging and therapy. Advanced Materials, 23(12), H18-H40.

Bouhelier, A., Bachelot, R., Lerondel, G., Kostcheev, S., Royer, P., & Wiederrecht, G. P. (2005). Surface Plasmon Characteristics of Tunable Photoluminescence in Single Gold Nanorods. Physical Review Letters, 95(26), 267405.

Cho, E. C., Zhang, Q., & Xia, Y. (2011). The effect of sedimentation and diffusion on cellular uptake of gold nanoparticles. Nat Nanotechnol, 6(6), 385-391. doi: 10.1038/nnano.2011.58

Davoren, M., Herzog, E., Casey, A., Cottineau, B., Chambers, G., Byrne, H. J., & Lyng, F. M. (2007). In vitro toxicity evaluation of single walled carbon nanotubes on human A549 lung cells. Toxicology in vitro, 21(3), 438-448.

Ejima, H., Richardson, J. J., Liang, K., Best, J. P., van Koeverden, M. P., Such, G. K., . . . Caruso, F. (2013). One-step assembly of coordination complexes for versatile film and particle engineering. Science, 341(6142), 154-157. doi: 10.1126/science.1237265

Fuguet, E., Ràfols, C., Rosés, M., & Bosch, E. (2005). Critical micelle concentration of surfactants in aqueous buffered and unbuffered systems. Analytica Chimica Acta, 548(1), 95-100.

Goodman, C. M., McCusker, C. D., Yilmaz, T., & Rotello, V. M. (2004). Toxicity of Gold Nanoparticles Functionalized with Cationic and Anionic Side Chains. Bioconjugate Chemistry, 15(4), 897-900. doi: 10.1021/bc049951i

Grabinski, C., Schaeublin, N., Wijaya, A., D'Couto, H., Baxamusa, S. H., Hamad-Schifferli, K., & Hussain, S. M. (2011). Effect of gold nanorod surface chemistry on cellular response. ACS Nano, 5(4), 2870-2879. doi: 10.1021/nn103476x

Huang, X., El-Sayed, I. H., Qian, W., & El-Sayed, M. A. (2006). Cancer Cell Imaging and Photothermal Therapy in the Near-Infrared Region by Using Gold Nanorods. Journal of the American Chemical Society, 128(6), 2115-2120. doi: 10.1021/ja057254a

Jun, T., Yong-Hua, L., Rong-Sheng, Z., Kai-Qun, L., Zhi-Guo, X., Zhao-Feng, L., . . . Hai, M. (2008). Effect of Aspect Ratio Distribution on Localized Surface Plasmon Resonance Extinction Spectrum of Gold Nanorods. Chinese Physics Letters, 25(12), 4459.

Nagesha, D., Laevsky, G. S., Lampton, P., Banyal, R., Warner, C., DiMarzio, C., & Sridhar, S. (2007). In vitro imaging of embryonic stem cells using multiphoton luminescence of gold nanoparticles. Int J Nanomedicine, 2(4), 813-819.

Pandey, S., Shah, R., Mewada, A., Thakur, M., Oza, G., & Sharon, M. (2013). Gold nanorods mediated controlled release of doxorubicin: nano-needles for efficient drug delivery. J Mater Sci Mater Med, 24(7), 1671-1681. doi: 10.1007/s10856-013-4915-4

Park, K., & Vaia, R. A. (2008). Synthesis of Complex Au/Ag Nanorods by Controlled Overgrowth. Advanced Materials, 20(20), 3882-3886. doi: 10.1002/adma.200800613

Pissuwan, D., Valenzuela, S., & Cortie, M. B. (2008). Prospects for gold nanorod particles in diagnostic and therapeutic applications. Biotechnol Genet Eng Rev, 25, 93-112.

Quirion, F., & Magid, L. J. (1986). Growth and counterion binding of cetyltrimethylammonium bromide aggregates at 25.degree.C: a neutron and light scattering study. The Journal of Physical Chemistry, 90(21), 5435-5441. doi: 10.1021/j100412a108

Schaeublin, N. M., Braydich-Stolle, L. K., Schrand, A. M., Miller, J. M., Hutchison, J., Schlager, J. J., & Hussain, S. M. (2011). Surface charge of gold nanoparticles mediates mechanism of toxicity. Nanoscale, 3(2), 410-420. doi: 10.1039/c0nr00478b

Sepúlveda, B., Angelomé, P. C., Lechuga, L. M., & Liz-Marzán, L. M. (2009). LSPR-based nanobiosensors. Nano Today, 4(3), 244-251. doi: 10.1016/j.nantod.2009.04.001

Untener, E. A., Comfort, K. K., Maurer, E. I., Grabinski, C. M., Comfort, D. A., & Hussain, S. M. (2013). Tannic acid coated gold nanorods demonstrate a distinctive form of endosomal uptake and unique distribution within cells. ACS Appl Mater Interfaces, 5(17), 8366-8373. doi: 10.1021/am402848q

Wan, J., Wang, J.-H., Liu, T., Xie, Z., Yu, X.-F., & Li, W. (2015). Surface chemistry but not aspect ratio mediates the biological toxicity of gold nanorods in vitro and in vivo. Sci. Rep., 5. doi: 10.1038/srep11398

Wang, L., Liu, Y., Li, W., Jiang, X., Ji, Y., Wu, X., . . . Chen, C. (2011). Selective targeting of gold nanorods at the mitochondria of cancer cells: implications for cancer therapy. *Nano Lett, 11*(2), 772-780. doi: 10.1021/nl103992v

Wijaya, A., Schaffer, S. B., Pallares, I. G., & Hamad-Schifferli, K. (2009). Selective release of multiple DNA oligonucleotides from gold nanorods. ACS Nano, 3(1), 80-86. doi: 10.1021/nn800702n

Yu, C., & Irudayaraj, J. (2006). Multiplex Biosensor Using Gold Nanorods. Analytical Chemistry, 79(2), 572-579. doi: 10.1021/ac061730d

LIST OF ACRONYMS

ATCC	American Type Culture Collection
AR	Aspect Ratio
CTAB	Cetyl trimethylammonium Bromide
DLS	Dynamic Light Scattering
FBS	Fetal Bovine Serum
GNMs	Gold Nanomaterials
GNRs	Gold Nanorods
HIS	Hyperspectral Imaging
ICP-MS	Inductively Coupled Plasma Mass Spectrometry
LCDC	Live Cell Dead Cell
MTAB	11-mercaptohexadecyl trimethylammonium Bromide
MTS	(3-(4,5-dimethylthiazol-2-yl)-5-(3-carboxymethoxyphenyl)-2-(4-sulfophenyl)-2H-tetrazolium)
NIR	Near-Infrared
NM	Nanomaterial
PBS	Phosphate Buffered Saline
PEG	Polyethylene glycol
ROS	Oxygen Species
SPR	Surface Plasmon Resonance
TA	Tannic Acid
TEM	Transmission Electron Microscopy
UV-Vis	Ultra-Violet Visible Spectroscopy